

1           **The changing character of twenty-first century precipitation over the**  
2           **western United States in the variable-resolution CESM**

3           Xingying Huang, \* Paul A. Ullrich

4           *Department of Land, Air and Water Resources, University of California, Davis*

5           \*Corresponding author address: Xingying Huang, Department of Land, Air and Water Resources,  
6           University of California Davis, Davis, CA 95616.  
7           E-mail: xyhuang@ucdavis.edu

## ABSTRACT

8 (To be added once the main content settled down)

9     **1. Introduction**

10    Understanding the character of precipitation within a changing climate has a major focus of  
11    climate science, primarily due to the pronounced impacts of water availability on socioeconomic  
12    and natural systems (???). Among these studies, there has been particular interest in precipitation  
13    extremes, which are manifested as drought and heavy precipitation events (?). Studies examining  
14    the character of precipitation in a warming world, which utilize models of varying complexity  
15    from simple thermodynamic models through complex coupled climate simulations, suggest that  
16    although atmospheric water vapor is increasing, the associated impacts of increased atmospheric  
17    water vapor on precipitation are far more complicated. Extreme precipitation events are even more  
18    nuanced: Some studies suggest that the intensity of extreme precipitation is projected to increase  
19    under global warming in many parts of the world, even in the regions where mean precipitation  
20    decreases (??).

21    Although future climate predictions are known to be often associated with large uncertainties,  
22    climate models are nonetheless one of the most useful tools for studying climate variability and  
23    extremes events in the future (?). Global climate models (GCMs) are often used to investigate  
24    possible future changes in the mean, variability and extremes of climate, typically forced with  
25    predicted greenhouse gas (GHGs) concentrations and aerosol emissions. Precipitation extremes,  
26    as measured by various metrics, are predicted to change by future warming based on the results of  
27    these simulations (?). Several past studies have investigated global impacts (?), but impacts at local  
28    and regional scales are more difficult to come by. Although increased GHG concentrations have  
29    contributed to observed intensification of heavy precipitation events over the tropical ocean (?)  
30    and the majority of Northern Hemisphere overland areas ?, these impacts are much more poorly

<sup>31</sup> understood at regional scales due to atmospheric circulation patterns of variability (?), which are  
<sup>32</sup> more difficult to assess at the coarse model resolutions used in previous studies.

<sup>33</sup> Insufficient regional-scale climate information has been a major outstanding problem in climate  
<sup>34</sup> science, as stakeholders and water managers typically require fine-scale information on climate  
<sup>35</sup> impacts in order to effectively develop adaptation and mitigation strategies. In order to reach the  
<sup>36</sup> scales needed for effective local planning, dynamical downscaling with regional climate models  
<sup>37</sup> (RCMs) has been typically used to ascertain the frequency, intensity, and duration of extreme  
<sup>38</sup> events. By only simulating a limited regional domain, RCMs better capture fine-scale dynamical  
<sup>39</sup> features under high horizontal resolution (????). Higher resolution can also enable more accurate  
<sup>40</sup> simulations of precipitation extremes, which can be driven by land use, land/water contrast, snow  
<sup>41</sup> cover, cloudiness and circulation patterns associated with topography (????). ? studied both heat  
<sup>42</sup> events and wet events over the contiguous United States based on RCMs simulation at 25 km hori-  
<sup>43</sup> zontal resolution, and demonstrated that fine-scale processes are critical for accurate assessment of  
<sup>44</sup> local- and regional-scale climate change vulnerability. ? showed that the higher-resolution nests  
<sup>45</sup> utilized by RCMs yield more realistic precipitation patterns and produce more frequent heavy  
<sup>46</sup> precipitation over the western U.S. (WUS), which is in turn more consistent with observations.

<sup>47</sup> Despite their success, RCMs also have known issues associated with inconsistency between the  
<sup>48</sup> lateral forcing data and the driven RCM, and the menu of physical parameterizations typically  
<sup>49</sup> available to RCMs expose the potential for over-tuning the model for a particular geographic  
<sup>50</sup> region (???). Consequently, there has been growing interest in variable-resolution enabled GCMs  
<sup>51</sup> (VRGCMs) to improve regional climate simulations. Unlike RCMs, which require GCM data  
<sup>52</sup> to drive the simulation at lateral boundaries, VRGCMs use a unified model with coarse global  
<sup>53</sup> resolution and enhanced resolution over a specific study region (??). VRGCMs have demonstrated

54 comparable utility for regional climate studies at a reduced computational cost, particular when  
55 compared to uniform-resolution GCMs (??).

56 In this paper, we utilize the recently developed variable-resolution option in the Community  
57 Earth System Model (VR-CESM). VR-CESM is based on the CESM (and its predecessor, the  
58 Community Climate System Model (CCSM)), a family of models that have been used for decades  
59 to study the global climate (??), and demonstrated competitive ability when contrasted with other  
60 climate models. The overall performance of VR-CESM for modeling regional climate in the Cali-  
61 fornia and Nevada is detailed in ?, who argued VR-CESM has competitive biases in comparison to  
62 the Weather Research and Forecasting (WRF) model (a traditional RCM), when evaluating both  
63 against high-quality observations and reanalysis. VR-CESM has also been employed for other  
64 studies and demonstrated that it is competitive at capturing fine-scale atmospheric processes with  
65 the uniform-resolution CESM and other RCMs, without apparent artifacts within the coarse-fine  
66 transition region (???).

67 This study focuses changes in the character of precipitation over the 21st Century within the  
68 WUS, as predicted from long-term ensemble runs conducted with VR-CESM with a local grid  
69 resolution of  $\sim 0.25^\circ$ . The WUS is known to be particularly vulnerable to hydrological extreme  
70 events, particularly floods and droughts (??), and features a variety of local features and micro-  
71 climates associated with its rough and varied topography. Simulations of the future climate are  
72 performed in accordance with the representative concentration pathway (RCP) 8.5 scenario, which  
73 describes a “business-as-usual” projection for GHGs among other RCPs (?). RCP 8.5 is a baseline  
74 scenario with updated base year calibration (to 2005) and no explicit climate policy (?) and end-  
75 of-century projections with the substantially weaker RCP2.6 scenario are found to be qualitatively  
76 similar to mid-century RCP8.5 results. Simulations are further conducted in accordance with the  
77 Atmospheric Model Intercomparison Project (AMIP) protocol (?), a widely-used approach for

78 climate model diagnosis, validation and intercomparison that imposes global sea surface temper-  
79 atures (SSTs) and sea ice. By constraining atmospheric boundary conditions at the sea surface,  
80 we avoid model biases that are known to exist in the fully coupled configuration (??) and accept  
81 potential uncertainties associated with our choice of SSTs.

82 Changes in the character of precipitation, in terms of frequency and intensity, have been assessed  
83 in our study from recent history through the end of 21st century. A comprehensive set of metrics  
84 for precipitation extremes have been evaluated from ensemble simulations over the **26-year** peri-  
85 ods corresponding to historical (1980-2005), mid-century (2025-2050) and end-of-century (2075-  
86 2100). Using this information, it is our goal to improve our understanding of precipitation at  
87 relatively fine spatial scales. We hypothesize that spatial inhomogeneity in local geography and  
88 temperature will also result in similarly inhomogeneous impacts on the precipitation field. We fur-  
89 ther expect that teleconnections (specifically the El Niño-Southern Oscillation (ENSO)) will have  
90 a pronounced impact on precipitation features over particular area under the changes of mean SST  
91 and its variations. Since only one SST dataset was used for this study, we note that our projections  
92 are conditioned on a particular future character of ENSO. This is a potentially large source of  
93 uncertainty, as at present there is no clear consensus on how ENSO may behave under a warming  
94 climate (??), and strengthening or weakening of this pattern will have clear consequences for our  
95 results.

96 This work builds on a number of previous studies that have explored the projected future change  
97 in WUS precipitation. For example, ? applied downscaled climate change signals to selected indi-  
98 cators, and concluded that global warming induced by increased CO<sub>2</sub> is likely to drive increases in  
99 extreme hydrologic events in the WUS. ? found that mean precipitation predicted by the RCMs are  
100 not statistically significant compared to interannual variability in many regions over WUS, though  
101 there is little consistency among the different RCMs as to responses in precipitation to increased

<sup>102</sup> **GHGs.** ? pointed out a potentially large increase in atmospheric river events by the end of the 21st  
<sup>103</sup> century under the RCP8.5 scenario.

<sup>104</sup> This paper is structured as follows. Section ?? describes the model setup. Section ?? describes  
<sup>105</sup> the methodology and reference datasets employed. An assessment of the ability of the model to  
<sup>106</sup> capture the climatology of the WUS is given in section ?? . Results from the future mean climatol-  
<sup>107</sup> ogy trend and projected changes to precipitation indices is in section ?? . Section ?? summarizes  
<sup>108</sup> the main points of the study along with further discussions.

## <sup>109</sup> **2. Model Setup**

<sup>110</sup> CESM is a state-of-the-art Earth modeling framework, consisting of coupled atmosphere, ocean,  
<sup>111</sup> land and sea ice models (??). In this study, Community Atmosphere Model version 5 (CAM5) (?)  
<sup>112</sup> and the Community Land Model version 4.0 (?) are used. Within CAM5, we use the Spectral  
<sup>113</sup> Element (SE) dynamical core, which incorporates the variable-resolution option (?) and includes  
<sup>114</sup> desirable conservation and parallel scalability properties (??). CLM is employed in the *unigrid*  
<sup>115</sup> configuration, which allows the land model to be co-located with the atmospheric grid and so elim-  
<sup>116</sup> inates the need for interpolation. SSTs and sea ice, which are used to compute ocean-atmosphere  
<sup>117</sup> fluxes, are prescribed in accordance with the AMIP protocol (?). The variable-resolution mesh  
<sup>118</sup> used for this study is depicted in Figure ??, in accord with our past studies (???).

<sup>119</sup> Simulations have been performed for the historical period (1979-2005, hereafter referred to as  
<sup>120</sup> hist) and for two future periods: 2024-2050 (hereafter referred to as mid) and 2074-2100 (hereafter  
<sup>121</sup> referred to as end). For purposes of analysis, the first year of each time period was discarded as a  
<sup>122</sup> spin-up period to allow adequate time for the initialized land and atmosphere to equilibrate. The  
<sup>123</sup> 26-year duration was chosen to provide an adequate sampling of annual variability for each time  
<sup>124</sup> phase. For future projections, GHG concentrations are set based on RCP8.5. Historical SSTs

125 and sea ice are prescribed at  $1^{\circ}$  resolution, as described by ?. SSTs and sea ice for each future  
126 period are developed from fully-coupled RCP 8.5 climate simulations with bias correction applied  
127 (Cecile Hannay, personal communication). Using prescribed SSTs in place of a coupled ocean  
128 model considerably reduces the computation cost and so allows the atmospheric model to be run  
129 at a higher overall resolution. Annually-updated land surface datasets, which prescribe land-use  
130 characteristics, are interpolated from  $0.5^{\circ}$  to the land model grid.

131 Ensemble runs are needed to ensure that the sample adequately accounts for climate variability,  
132 especially for statistics associated with climatological extremes. However, the exact number of en-  
133 semble members required is heavily dependent on the variability of the particular metric being ex-  
134 amined, and so no standard ensemble criteria exists (?). ? suggest that around 3 ensemble runs are  
135 required to detect a significant epoch difference for JJA (June-July-August) surface temperatures,  
136 whereas 10 to 30 ensemble members are needed for that for DJF (Dec.-Jan.-Feb.) precipitation.  
137 In our study, the use of prescribed SSTs does reduce the intrinsic variability of the climate system  
138 (see supplement), and so we found reasonably converged results with two ensemble members for  
139 the historical period and four ensemble members for each future period.

### 140 3. Methodology

#### 141 a. Precipitation indices

142 In order to fully account for the precipitation distributions, daily output over all the years are uti-  
143 lized in data analysis. We have employed standard indices to characterize precipitation (???). Sev-  
144 eral indices have been examined, including those defined by the Expert Team on Climate Change  
145 Detection and Indices (ETCCDI) (?) that have been primarily adopted in previous studies (????)  
146 and others such as return levels, dry spell and wet spell defined by either percentiles or by selected

<sup>147</sup> **thresholds.** As a result, loosely based on the former studies, the indices we have chosen for this  
<sup>148</sup> study attempt to provide a relatively comprehensive characterization of precipitation, along with  
<sup>149</sup> being easy to interpret and relevant to stakeholders. The indices employed are summarized in  
<sup>150</sup> Table ??.

<sup>151</sup> *b. Impacts of ENSO*

<sup>152</sup> The impact of ENSO on precipitation is emphasized in our study due to its impact in regulating  
<sup>153</sup> the precipitation over a majority of our study area, particularly in the southwest U.S. (????). The  
<sup>154</sup> phase of ENSO (*i.e.* El Niño and La Niña) is identified each year using the Oceanic Niño Index  
<sup>155</sup> (ONI), defined as the 3-month running means of SST anomalies in the Niño 3.4 region (covering  
<sup>156</sup> 5N-5S, 120-170W based on ?). An El Niño or La Niña episode is said to occur when the ONI  
<sup>157</sup> exceeds +0.5 or -0.5 for at least five consecutive months (?) (see the supplement). In order  
<sup>158</sup> to remove the trend in the SST field associated with climate change, the anomaly is computed  
<sup>159</sup> against the detrended mean SSTs from the periods 1971-2000, 2020-2050 and 2070-2100 for hist,  
<sup>160</sup> mid and end respectively, using the aforementioned observed and predicted SST datasets. We  
<sup>161</sup> have also tried to use wider ranges (from 105W to 170W) than 3.4 region (from 120W to 170W)  
<sup>162</sup> to recalculate the SST anomaly as argued by some studies for different types of ENSO (?), and the  
<sup>163</sup> results are statistically the same as using Niño 3.4.

<sup>164</sup> Student's t-test has been used to test whether or not two datasets at each grid point are statis-  
<sup>165</sup> tically equivalent, if the sample population can be adequately described by a normal distribution.  
<sup>166</sup> The normality of a dataset is assessed under the Anderson-Darling test. When the sample popu-  
<sup>167</sup> lations do not approximately follow a normal distribution, Mann-Whitney-Wilcoxon (MWW) test  
<sup>168</sup> is employed in lieu of the t-test. All these tests are evaluated at the 0.05 ( $\alpha$ ) significance level.  
<sup>169</sup> (add description of the supplement like what are included)

170 *c. Reference datasets*

171 Gridded observational datasets and reanalysis of the highest available quality with comparable  
172 horizontal resolutions to our VR-CESM simulations are used for assessing the simulation qual-  
173 ity. The use of multiple reference datasets is necessary due to the underlying uncertainty in the  
174 reference data. Descriptions of the datasets employed are as follows.

175 **UW Precipitation Dataset:** The UW daily gridded meteorological data is obtained from  
176 the Surface Water Modeling group at the University of Washington (??). UW incorporates  
177 topographic corrections for the precipitation. The dataset is provided at  $0.125^{\circ}$  horizontal  
178 resolution covering the period 1949 to 2010.

179 **NCEP CPC:** This dataset provides gauge-based analysis of daily precipitation from the Na-  
180 tional Oceanic and Atmospheric Administration (NOAA) Climate Prediction Center (CPC).  
181 It is a suite of unified precipitation products obtained by combining all information avail-  
182 able at CPC via the optimal interpolation objective analysis technique. The gauge analysis  
183 covers the Conterminous United States with a fine-resolution at  $0.25^{\circ}$  from 1948-01-01 to  
184 2006-12-31.

185 **North American Regional Reanalysis (NARR):** The is the NCEP (National Centers for En-  
186 vironmental Prediction) high-resolution reanalysis product that provides dynamically down-  
187 scaled data over North America at  $\sim 32$  km resolution and 3-hourly intervals from 1979  
188 through present (?).

189 **4. Model Assessment**

190 Before proceeding, we first investigate how well the model is able to represent the character of  
191 precipitation over the WUS. Figures ?? and Figure ?? depict the spatial character of the indices

192 defined in Table ???. Considering the uncertainty within the reference datasets, the mean of the ref-  
193 erences are used to get the difference from the model output. T-test is applied here with UW, CPC  
194 and NARR as the three statistical samples and the historical runs as two samples averaged over  
195 the whole period, determining at each spatial point whether VR-CESM is statistically equivalent  
196 to the references as stippled in ?? and ??.

197 Compared with observations, VR-CESM well represents the spatial pattern of precipitation, with  
198 majority of the precipitation distributed along the northwest coastal area and the mountainous re-  
199 gions of the Cascades and the Sierra Nevada. Compared to the mean of the references, VR-CESM  
200 does overestimate the Pr significantly over most of the relatively dry region for about 0.2 mm to  
201 1.5 mm, especially over the eastern side of the Cascades and both sides of the Sierra Nevada (with  
202 relatively difference reaching 50%-150%). This is further reflected in the overestimation of the  
203 non-extreme Pr events frequency (with  $Pr < 10\text{mm/day}$ ) since most precipitation over dry area  
204 is associated with low rainy rate days. However, for the western flank of the Sierra Nevada, the  
205 overestimation of the mean Pr is mainly due to the intensified rain rate, which may related with  
206 the strengthened treatment of orographic effects with excessively strong upward winds. Nonethe-  
207 less, the model captures the precipitation features including frequency and intensity satisfactorily  
208 over the main wet region, where most precipitation is resulted from extreme Pr events (when  
209  $Pr > 10\text{mm/day}$ ), without significant difference.

210 The corresponding contribution fraction to total precipitation amount of each range defined in  
211 our metrics is also well represented in the model without significant difference, except the western  
212 side of the the Sierra Nevada and eastern flank of the Cascades in the Washington. This sug-  
213 gests that despite the aforementioned biases, VR-CESM can still capture the overall shape of the  
214 precipitation distributions. Biases in simulating extreme precipitation over the topographically  
215 complex regions including the Cascades and Sierra Nevada ranges have also been found by in the

216 high-resolution simulation by RCMs ??, and have been primarily attributed to excessively strong  
217 winds. Biases with the excessively dry eastern flanks of these mountains may also be associated  
218 with the prognostic treatment of precipitation species in CESM.

219 As further supported in ? by evaluating VR-CESM also at  $0.25^{\circ}$  for long-term regional climate  
220 modeling over California, it is found that VR-CESM can adequately represented regional climatic  
221ological patterns with high spatial correlations. VR-CESM shows comparable performance as  
222 WRF at 27 km, but still overestimated overall winter precipitation (about 25%-35%) compared  
223 to reference datasets, with statistically significant difference over the western edge of the Sierra  
224 Nevada, which can be alleviated by increasing the spatial resolution due to improved treatment  
225 of orographic effects. The spatial pattern of variability agrees well between VR-CESM and refer-  
226 ences and when assessing the frequency of strong precipitation events, VR-CESM matched closely  
227 to the UW dataset everywhere except the Central Valley.

228 CESM at 1 degree resolution was also assessed in order to better understand the impacts of reso-  
229 lution. We find that precipitation patterns over complex topography are poorly represented without  
230 capturing the spatial patterns induced by orographic effects over the Cascades and Sierra Nevada  
231 by uniform CESM at 1 degree, with total precipitation greatly underestimated, when compared to  
232 VR-CESM, gridded data and reanalysis (see the supplement). Basically, the precipitation has been  
233 smooth out at the coastal area and the mountainous regions over northwest U.S when simulated  
234 with CESM at coarse resolution. This result clearly captures the benefits of high resolution (par-  
235 ticularly the representation of topography) in simulating precipitation features. Results are also  
236 provided for the output from a globally uniform CESM run at  $0.25^{\circ}$  spatial resolution with the  
237 finite volume (FV) dynamical core (?), exhibiting comparable performance to VR-CESM (see the  
238 supplement).

239 (For the t-test among different time periods, I use the yearly values of each run.)

240 **5. Drivers of climatological precipitation**

241 [To be filled in based on earlier discussion based on the literature]

242 [Increased temperatures will lead to higher water vapor content over the ocean, in accordance  
243 with C-C. Evaporation over the ocean will increase, but may be limited over land due to limitations  
244 on soil moisture. The storm track may be enhanced, which would increase large-scale precipitation  
245 events (ARs) along the U.S. west coast.]

246 **6. Results**

247 *a. Mean climatology*

248 Before proceeding with the analysis of precipitation features, it is first important to understand  
249 how the mean climatology changes in VR-CESM across time periods (Figure ??). Since the  
250 character of WUS precipitation has a strong seasonal dependence, the mean climatology including  
251 mean precipitation, near-surface temperature and near-surface relative humidity are depicted in  
252 two seasons including the cool season (or wet season) from October to March and the warm  
253 season (or dry season) from April to September.

254 As a result of enhanced GHG concentrations, mean annual temperature increases by about 1.5 to  
2 K from hist to mid and about 4 to 6 K from mid to end. Despite the large spatial variation in cli-  
255 matological temperatures, the temperature change between historical and future is fairly uniform.  
256 However, there is a slightly weaker increase in the near-coastal regions during cool season and in  
257 the lower latitude area at warm season, which might be due to the increased westerly wind during  
258 cool seasons and northward wind during warm season from the near ocean. Larger increases of  
259 temperature is also observed in warm season than cool season for about 0.5 K and 1 K for mid and  
260 end respectively.

262 As described by the Clausius-Clapeyron (C-C) equation, the water vapor content is supposed to  
263 increase by  $\sim 7\%$  for each  $1^{\circ}\text{C}$  increase in temperature. With the increase of the temperature in  
264 future, water vapor evaporation will increase over the ocean. Practically, whether the increase rate  
265 of the water vapor as the temperature goes up will keep the same or not will directly affect the rel-  
266 ative humidity. As water vapor reaches saturation, condensation triggers clouds and precipitation.  
267 However, when the air holds more water vapor, the chances of heavy rain events tend to increase  
268 even when even where total precipitation is decreasing (?). To understand the increasing rate of  
269 water vapor content under climate warming and whether relative humidity can be remain or not,  
270 2m relative humidity (RH) is plotted in Figure ??.

271 Overall, RH remains almost the same as hist over the regions where temperature does not sub-  
272 stantially increase. However, in regions where temperature increase is larger than 2 K, RH is  
273 instead observed to decrease significantly relative to historical values for about 2% and 3-6%  
274 compared to mid and end respectively. In fact, trends in RH are spatially consistent with tempera-  
275 ture increase but opposite in magnitude with a spatial correlation coefficient of approximately 0.8.  
276 This suggests that continental evaporation and water vapor transport is insufficient to compensate  
277 for the air vapor capacity when temperature increases to certain level, which is consistent with  
278 ?, and has been observed in results by ? over continental and southeastern Europe and ? over  
279 low-latitude and midlatitude land areas.

280 Based on those background changes of heat and water vapor, from hist to mid, mean precipita-  
281 tion showed a 0.2-0.6 mm/day increase during cool season with a largest change over northwest  
282 and less than 0.2 mm/day during warm season over southeast part. From hist to end, the increase  
283 is about 0.4-1.2 mm/day during cool season with also a largest change over northwest, and no  
284 notable change is observed during warm season. Nonetheless, these results are statistically sig-  
285 nificant (see Figure ??) (how about add significance here)? East of the Rockies, precipitation

increases through mid-century (statistically significant), but this trend appears to recede towards the end of the century (although these results are not significant). There is also a decrease of about 0.1mm/day in total precipitation over the western flank of the Sierra Nevadas during the cool season from hist to future. This decrease (about 0.15 mm/day) is also found over the Cascades and the western coastal area during warm season from hist to mid. However, this decrease is not statistically significant. Majority of the precipitation over the cool season emerged from large-scale patterns, whereas warm season precipitation was from convection processes.

The precipitation over WUS for moderate or heavy precipitation is mainly resulted from the large-scale water flux transport from the eastern Pacific Ocean rather than directly from evaporation, mainly in the form of atmospheric rivers or orographic updraft (??). According to previous studies (e.g. (????)), changes in more extreme precipitation follow the C-C relationship more closely than total precipitation precipitation amount (?). In order to find out the precipitation changes in a comprehensive aspect based on our fine-scale simulations, analyses of different precipitation distributions are focused in the following part to account for the future changes of diverse precipitation events.

### *b. Precipitation indices*

We now turn our attention to the precipitation indices presented in Table ???. For each index, the changes of precipitation character for each period, averaged over all ensemble members are plotted in Figure ?? (for the indices that quantify precipitation days) and Figure ?? (for the indices describing precipitation amounts). Although mean precipitation shows a weak but overall increasing trend from hist to mid and mid to end, the precipitation indices exhibit substantially more unique character.

308 When comparing `hist` to `mid`, the total rainy days and frequency of non-extreme precipitation  
309 have significantly increased mainly over the central-east and southeast part of WUS, which is  
310 not observed between `mid` and `end`. On the contrary, the total rainy days and frequency of non-  
311 extreme precipitation have decreased significantly over the northwest region and the eastern part  
312 of the Montana, Wyoming and Oregon from `mid` to `end`. These changes are the primary driver for  
313 the observed change to mean precipitation exhibited in Figure ??.

314 As for extreme precipitation frequency (i.e. days with daily Pr between 10 mm and 40 mm),  
315 the number of days increases from `hist` to `mid`, but the pattern of is scattered over northwest and  
316 central WUS. When comparing `mid` to `end`, there is a clear and significant increase in extreme  
317 precipitation events over the northwest coastal area and eastern flank of the Cascades. This result  
318 is consistent with ?, who observe a robust increase in winter precipitation extremes toward the  
319 latter half of the 21st century using RCMs [an ensemble of RCMs?].

320 There is a slight, but insignificant decrease over the Cascades and the Sierra Nevada (significance  
321 is low due to the high variability of precipitation). For very extreme precipitation ( $\text{Pr} >= 40 \text{ mm}$ )  
322 events, there is an increasing trend over the northwest coast and the Cascades and its eastern  
323 flank. The corresponding changes in rain amount are consistent with the changes of frequency  
324 (see Figure ??). Overall, these results indicate more extreme precipitation over the northwest U.S.

325 (might add the specific percentages for further illustrations)

326 [Why does Fig. 8 appear before Fig. 7?] In order to understand the drivers behind the observed  
327 changes, we first examine change in moisture flux for cool seasons when WUS precipitation is  
328 primarily from water vapor influx from the Pacific Ocean (see Figure ??). Examining the moisture  
329 flux at 850 hPa, we observe an increase in specific humidity that accompanies the increase of the  
330 temperature in future [where is this observed? not in Fig. 8]. However, when comparing to `hist`,  
331 wind patterns in `mid` and `end` are also reduced over the eastern part of the WUS and enhanced

332 to the west [where? I don't see it]. [These previous several sentences require some clarification  
333 as I don't see what you are referring to] Integrated vapor transport (IVT) (Figure ??) for extreme  
334 precipitation days over cool seasons. Generally, IVT is useful to understand extreme precipitation  
335 events that arise from atmospheric rivers over the northwestern U.S. and from orographic uplift  
336 (especially for very extreme precipitation) (???). Based on the observed change in IVT, it is clear  
337 that the increase in moisture influx from past to future, which is mainly due to the change of the  
338 air water vapor content with increased temperature, corresponds to the changes of precipitation  
339 extremes shown in Figure ??.

## 340 1) QUANTILE CORRELATION ANALYSIS

341 [Motivating question: Can changes in mean precipitation be used to predict changes in extreme  
342 precipitation?]

## 343 2) ISOLATING DIFFERENCES DUE TO CLIMATE CHANGE AND ENSO

344 [Motivate] The phase of ENSO is well known to have important repercussions on precipitation  
345 extremes [citation needed]. ENSO from past to future, the difference of precipitation behaviors  
346 between the warm phase (i.e. El Niño) and cool phase (i.e. La Niña) of ENSO is illustrated in  
347 Figure ?? for the wet seasons of each time period. Based on the ONI index values, the mean SST  
348 anomalies are 1.38, 1.71 and 2.30 K during El Niño years, and -1.16, -1.62 and -1.43 K during La  
349 Niña years for hist, mid and end respectively [some references are needed to place this behavior  
350 of ENSO within the context of the literature – are these values reasonable?]. The SST anomalies  
351 of each year or each month [or?], and their associated spatial pattern when averaged during the  
352 warm and cool phases can be found in the supplement (might adding some descriptions of these).  
353 [Also include mean SSTs during each period]

354 [Fig. 7 shows a pronounced impact of ENSO through Northern California that seems uncharac-  
355 teristic of what I know about ENSO from the literature. I had thought ENSO primarily impacts  
356 Southern California. Discuss briefly?]

357 During the El Niño phase, intensified mean precipitation is expected over the southwest (?),  
358 along with reduced precipitation intensity over the northwest. This feature is characterized as  
359 a northwest/southwest precipitation dipole, triggered by ENSO's modification of the storm track  
360 (??), along with [?] modulation of the enhanced precipitation variability in the southern WUS (??).  
361 This dipole is also apparently in the frequency of rainy days and extreme precipitation events. In  
362 mid and hist, ENSO is observed to intensify, which appears to be related with the changes of  
363 the strength of El Niño and La Niña [Since ENSO behavior is strongly dependent on choice of  
364 climate model, you need to put this behavior in context and explain how a weakening ENSO could  
365 potentially impact these precipitation projections, which should emerge from the linear model  
366 result]. This can be explained by the SST anomaly magnitude (detrended) of warm and cold  
367 phases (see the supplement). ? also found a statistically significant linkages with ENSO and PDO  
368 for both the overall and extreme intensity of wintertime precipitation over the WUS using CCSM4  
369 (earlier form of CESM). Strengthening storm patterns associated with ENSO are also found by ?  
370 over California using CMIP5 output under RCP8.5.

371 [Do you want to discuss your observation of only a weak influence from PDO?]

372 [You should show the results of climatological change with changes due to ENSO removed]

373 (For Figure 7, might add percentage of changes)

374 The impact of ENSO is further observed by the IVT difference over rainy days between El Niño  
375 and La Niña (see Figure ??) accompanying by the wind pattern difference at 850 hPa, showing  
376 the increase of the moisture flux for the southwest and decrease for the northwest. However, the  
377 impact of ENSO for observational precipitation has a weaker signal of the dipole effect compared

378 to the VR-CESM (see the supplement), which might suggest that the model has a overestimation  
379 of ENSO's impact on precipitation, especially over the northwest U.S. The improvement of ENSO  
380 in the model is directly proportional to the representation of ENSO forced precipitation anomalies  
381 (?).

382 Based on the above results, it can be seen that the magnitude of the effects of ENSO is compara-  
383 ble or even higher than the impacts of climate forcing. For further investigation, linear regression  
384 is applied to signaling the factor effects due to ENSO and climate forcing. First, we get the SST  
385 anomaly of each year at each grid point over our study area followed by the way of Niño 3.4 to  
386 be the ENSO factor values. Then, we use the GHGs values at each year to represent the climate  
387 forcing factor. The features of the precipitation indices as we defined above are used as response  
388 variables. Combined the values of all the time period and all the runs, we got the significance of  
389 these two factors' effects at each grid point based on the ANOVA (analysis of variance) output.  
390 (see the supplement) (This is not complete yet, but not sure whether to add this or not).

391 add the correlation of the quantiles result here

## 392 7. Discussion and Summary

393 In this study, the North Pacific Oscillation (NPO) is not analyzed as its decadal duration mak-  
394 ing it difficult to capture within the 26 years simulation time period. Further, as argued by ?, the  
395 NPO does not respond to the same internal atmospheric variability as ENSO, and so no signifi-  
396 cant improvement [improvement in what?] can be obtained to account for the ENSO's effects by  
397 incorporating accurate predictions of NPO SSTs.

398 The associated precipitation signal under a warmer climate is more ambiguous for California  
399 (?) considering the extreme variability on interannual time scales (?). ? found that under global  
400 warming, heavy precipitation events show largest increases in the mountainous regions of the

401 northern California Coastal Range and the Sierra Nevada. However, our results show a minor  
402 decrease (though not statistically significant) of extreme precipitation over the Sierra Nevada.

403 Although, the strength of ENSO intensifies in the future with CESM, there is still substantial  
404 uncertainty regarding how El Niño will change under global warming by altering the background  
405 climate or not as debated by plenty of studies (??) [??]. There is still no clear agreement among  
406 coupled models whether ENSO will weaken or strengthen in response to increased greenhouse  
407 gas concentrations, particularly as ENSO appears to be relatively insensitive to a doubling of CO<sub>2</sub>  
408 in most models (?). However, correctly simulation changes to the spatial pattern of SSTs ion  
409 state-of-the-art coupled GCMs remains challenging ????. ? showed that the diversity of El Niño  
410 characteristics in CCSM4 is comparable to what was found in observations, although, as found by  
411 ?, the overall magnitude of ENSO in CCSM4 is overestimated by 30% over the preindustrial time  
412 period. ? assessed ENSO in CCSM4 (predating CESM) and observed no signal when comparing  
413 the twentieth and twenty-first-century ensembles, as also argued by ?. It is believed that large  
414 ensembles are needed to isolate a significant climate change response within ENSO, and inter-  
415 model teleconnection differences (?) [?].

416 The increased cool season precipitation extremes tend to result in higher runoff events over  
417 the northwest U.S., which are in turn associated with a greater chance of flooding and a loss of  
418 snowpack. A decrease in counts of rainy days during the warm season over central and southern  
419 California, though small in magnitude, will probably intensify the drought condition due to the  
420 deficit of soil moisture with higher evapotranspiration caused by the warmer climate in the future  
421 ??.

422 (Summary is to be added once the main content have been settled down)

423 *Acknowledgments.* The authors would like to thank Michael Wehner for sharing the dataset and  
424 many suggestions. The authors also want to thank Alan M. Rhoades for providing the simulation  
425 output. We acknowledge the substantial efforts behind the datasets used in this study, including  
426 UW, NCDC and NARR. The simulation data used is available by request at xyhuang@ucdavis.edu.  
427 This project is supported in part by the xxx and by the xxx.

428 **References**

- 429 AchutaRao, K., and K. R. Sperber, 2006: Enso simulation in coupled ocean-atmosphere models:  
430 are the current models better? *Climate Dynamics*, **27** (1), 1–15.
- 431 Allan, R. P., and B. J. Soden, 2008: Atmospheric warming and the amplification of precipitation  
432 extremes. *Science*, **321** (5895), 1481–1484.
- 433 Bell, J. L., L. C. Sloan, and M. A. Snyder, 2004: Regional changes in extreme climatic events: a  
434 future climate scenario. *Journal of Climate*, **17** (1), 81–87.
- 435 Caldwell, P., 2010: California wintertime precipitation bias in regional and global climate models.  
436 *Journal of Applied Meteorology and Climatology*, **49** (10), 2147–2158.
- 437 Capotondi, A., 2013: Enso diversity in the ncar ccsm4 climate model. *Journal of Geophysical  
438 Research: Oceans*, **118** (10), 4755–4770.
- 439 Cayan, D. R., T. Das, D. W. Pierce, T. P. Barnett, M. Tyree, and A. Gershunov, 2010: Future  
440 dryness in the southwest us and the hydrology of the early 21st century drought. *Proceedings of  
441 the National Academy of Sciences*, **107** (50), 21 271–21 276.
- 442 Cayan, D. R., K. T. Redmond, and L. G. Riddle, 1999: ENSO and hydrologic extremes in the  
443 western United States\*. *Journal of Climate*, **12** (9), 2881–2893.

- 444 DeFlorio, M. J., D. W. Pierce, D. R. Cayan, and A. J. Miller, 2013: Western us extreme precipita-  
445 tion events and their relation to enso and pdo in csm4. *Journal of Climate*, **26** (12), 4231–4243.
- 446 Dennis, J., and Coauthors, 2011: CAM-SE: A scalable spectral element dynamical core for the  
447 Community Atmosphere Model. *International Journal of High Performance Computing Appli-*  
448 *cations*, 1094342011428142.
- 449 Deser, C., R. Knutti, S. Solomon, and A. S. Phillips, 2012a: Communication of the role of natural  
450 variability in future north american climate. *Nature Climate Change*, **2** (11), 775–779.
- 451 Deser, C., A. Phillips, V. Bourdette, and H. Teng, 2012b: Uncertainty in climate change projec-  
452 tions: the role of internal variability. *Climate Dynamics*, **38** (3-4), 527–546.
- 453 Deser, C., and Coauthors, 2012c: Enso and pacific decadal variability in the community climate  
454 system model version 4. *Journal of Climate*, **25** (8), 2622–2651.
- 455 Dettinger, M., 2011: Climate change, atmospheric rivers, and floods in california—a multimodel  
456 analysis of storm frequency and magnitude changes1. Wiley Online Library.
- 457 Diffenbaugh, N. S., J. S. Pal, R. J. Trapp, and F. Giorgi, 2005: Fine-scale processes regulate the  
458 response of extreme events to global climate change. *Proceedings of the National Academy of*  
459 *Sciences of the United States of America*, **102** (44), 15 774–15 778.
- 460 DiNezio, P. N., B. P. Kirtman, A. C. Clement, S.-K. Lee, G. A. Vecchi, and A. Wittenberg, 2012:  
461 Mean climate controls on the simulated response of enso to increasing greenhouse gases. *Jour-*  
462 *nal of Climate*, **25** (21), 7399–7420.
- 463 Dominguez, F., E. Rivera, D. Lettenmaier, and C. Castro, 2012: Changes in winter precipitation  
464 extremes for the western united states under a warmer climate as simulated by regional climate  
465 models. *Geophysical Research Letters*, **39** (5).

- <sup>466</sup> Duffy, P., and Coauthors, 2006: Simulations of present and future climates in the western United States with four nested regional climate models. *Journal of Climate*, **19** (6), 873–895.
- <sup>467</sup>
- <sup>468</sup> Easterling, D. R., G. A. Meehl, C. Parmesan, S. A. Changnon, T. R. Karl, and L. O. Mearns, 2000: Climate extremes: observations, modeling, and impacts. *science*, **289** (5487), 2068–2074.
- <sup>469</sup>
- <sup>470</sup> Fedorov, A. V., and S. G. Philander, 2000: Is el niño changing? *Science*, **288** (5473), 1997–2002.
- <sup>471</sup>
- <sup>472</sup> Fox-Rabinovitz, M., J. Côté, B. Dugas, M. Déqué, and J. L. McGregor, 2006: Variable resolution general circulation models: Stretched-grid model intercomparison project (SGMIP). *Journal of Geophysical Research: Atmospheres (1984–2012)*, **111** (D16).
- <sup>473</sup>
- <sup>474</sup> Fox-Rabinovitz, M. S., G. L. Stenchikov, M. J. Suarez, and L. L. Takacs, 1997: A finite-difference GCM dynamical core with a variable-resolution stretched grid. *Monthly weather review*, **125** (11), 2943–2968.
- <sup>475</sup>
- <sup>476</sup>
- <sup>477</sup> Frei, C., R. Schöll, S. Fukutome, J. Schmidli, and P. L. Vidale, 2006: Future change of precipitation extremes in Europe: Intercomparison of scenarios from regional climate models. *Journal of Geophysical Research: Atmospheres (1984–2012)*, **111** (D6).
- <sup>478</sup>
- <sup>479</sup>
- <sup>480</sup> Gao, Y., J. Lu, L. R. Leung, Q. Yang, S. Hagos, and Y. Qian, 2015: Dynamical and thermodynamical modulations on future changes of landfalling atmospheric rivers over western north america. *Geophysical Research Letters*, **42** (17), 7179–7186.
- <sup>481</sup>
- <sup>482</sup>
- <sup>483</sup> Gates, W. L., 1992: AMIP: The Atmospheric Model Intercomparison Project. *Bulletin of the American Meteorological Society*, **73**, 1962–1970.
- <sup>484</sup>
- <sup>485</sup> Gershunov, A., and T. P. Barnett, 1998: Interdecadal modulation of enso teleconnections. *Bulletin of the American Meteorological Society*, **79** (12), 2715–2725.
- <sup>486</sup>

- 487 Guilyardi, E., A. Wittenberg, A. Fedorov, M. Collins, C. Wang, A. Capotondi, G. J. Van Olden-  
488 borg, and T. Stockdale, 2009: Understanding el ni  o in ocean-atmosphere general circulation  
489 models. *Bulletin of the American Meteorological Society*, **90** (3), 325.
- 490 Hamlet, A. F., and D. P. Lettenmaier, 2005: Production of Temporally Consistent Gridded Precipi-  
491 tation and Temperature Fields for the Continental United States\*. *Journal of Hydrometeorology*,  
492 **6** (3), 330–336.
- 493 Hamlet, A. F., and D. P. Lettenmaier, 2007: Effects of 20th century warming and climate variability  
494 on flood risk in the western us. *Water Resources Research*, **43** (6).
- 495 Hegerl, G. C., F. W. Zwiers, P. A. Stott, and V. V. Kharin, 2004: Detectability of anthropogenic  
496 changes in annual temperature and precipitation extremes. *Journal of Climate*, **17** (19), 3683–  
497 3700.
- 498 Huang, X., A. M. Rhoades, P. A. Ullrich, and C. M. Zarzycki, 2016: An evaluation of the vari-  
499 able resolution-cesm for modeling california’s climate. *Journal of Advances in Modeling Earth  
500 Systems*.
- 501 Hurrell, J. W., J. J. Hack, D. Shea, J. M. Caron, and J. Rosinski, 2008: A new sea surface temper-  
502 ature and sea ice boundary dataset for the Community Atmosphere Model. *Journal of Climate*,  
503 **21** (19), 5145–5153.
- 504 Hurrell, J. W., and Coauthors, 2013: The community earth system model: A framework for col-  
505 laborative research. *Bulletin of the American Meteorological Society*, **94** (9), 1339–1360.
- 506 Jha, B., Z.-Z. Hu, and A. Kumar, 2014: Sst and enso variability and change simulated in historical  
507 experiments of cmip5 models. *Climate dynamics*, **42** (7-8), 2113–2124.

- 508 Joseph, R., and S. Nigam, 2006: Enso evolution and teleconnections in ipcc's twentieth-century  
509 climate simulations: Realistic representation? *Journal of Climate*, **19** (17), 4360–4377.
- 510 Joshi, M. M., J. M. Gregory, M. J. Webb, D. M. Sexton, and T. C. Johns, 2008: Mechanisms for  
511 the land/sea warming contrast exhibited by simulations of climate change. *Climate Dynamics*,  
512 **30** (5), 455–465.
- 513 Kahya, E., and J. A. Dracup, 1994: The influences of type 1 el nino and la nina events on stream-  
514 flows in the pacific southwest of the united states. *Journal of Climate*, **7** (6), 965–976.
- 515 Kao, H.-Y., and J.-Y. Yu, 2009: Contrasting eastern-pacific and central-pacific types of enso.  
516 *Journal of Climate*, **22** (3), 615–632.
- 517 Kharin, V. V., F. W. Zwiers, X. Zhang, and G. C. Hegerl, 2007: Changes in temperature and  
518 precipitation extremes in the IPCC ensemble of global coupled model simulations. *Journal of*  
519 *Climate*, **20** (8), 1419–1444.
- 520 Kim, J., 2005: A projection of the effects of the climate change induced by increased co2 on  
521 extreme hydrologic events in the western us. *Climatic Change*, **68** (1-2), 153–168.
- 522 Laprise, R., and Coauthors, 2008: Challenging some tenets of regional climate modelling. *Meteo-*  
523 *rology and Atmospheric Physics*, **100** (1-4), 3–22.
- 524 Leung, L. R., L. O. Mearns, F. Giorgi, and R. L. Wilby, 2003a: Regional climate research: needs  
525 and opportunities. *Bulletin of the American Meteorological Society*, **84** (1), 89–95.
- 526 Leung, L. R., and Y. Qian, 2009: Atmospheric rivers induced heavy precipitation and flooding in  
527 the western US simulated by the WRF regional climate model. *Geophysical research letters*,  
528 **36** (3).

- 529 Leung, L. R., Y. Qian, and X. Bian, 2003b: Hydroclimate of the western United States based on  
530 observations and regional climate simulation of 1981-2000. Part I: Seasonal statistics. *Journal*  
531 *of Climate*, **16 (12)**, 1892–1911.
- 532 Maloney, E. D., and Coauthors, 2014: North american climate in cmip5 experiments: part iii:  
533 assessment of twenty-first-century projections\*. *Journal of Climate*, **27 (6)**, 2230–2270.
- 534 Maurer, E., A. Wood, J. Adam, D. Lettenmaier, and B. Nijssen, 2002: A long-term hydrologically  
535 based dataset of land surface fluxes and states for the conterminous United States\*. *Journal of*  
536 *climate*, **15 (22)**, 3237–3251.
- 537 McDonald, A., 2003: Transparent boundary conditions for the shallow-water equations: testing in  
538 a nested environment. *Monthly weather review*, **131 (4)**, 698–705.
- 539 Meehl, G. A., H. Teng, and G. Bannister, 2006: Future changes of el niño in two global coupled  
540 climate models. *Climate Dynamics*, **26 (6)**, 549–566.
- 541 Mesinger, F., and K. Veljovic, 2013: Limited area NWP and regional climate modeling: a test  
542 of the relaxation vs Eta lateral boundary conditions. *Meteorology and Atmospheric Physics*,  
543 **119 (1-2)**, 1–16.
- 544 Mesinger, F., and Coauthors, 2006: North American regional reanalysis. *Bulletin of the American*  
545 *Meteorological Society*, **87**, 343–360.
- 546 Min, S.-K., X. Zhang, F. W. Zwiers, and G. C. Hegerl, 2011: Human contribution to more-intense  
547 precipitation extremes. *Nature*, **470 (7334)**, 378–381.
- 548 Neale, R. B., and Coauthors, 2010a: Description of the NCAR community atmosphere model  
549 (CAM 5.0). *NCAR Tech. Note NCAR/TN-486+ STR*.

550 Neale, R. B., and Coauthors, 2010b: Description of the NCAR Community Atmosphere Model  
551 (CAM 5.0). NCAR Technical Note NCAR/TN-486+STR, National Center for Atmospheric Re-  
552 search, Boulder, Colorado, 268 pp.

553 Neelin, J. D., B. Langenbrunner, J. E. Meyerson, A. Hall, and N. Berg, 2013: California winter  
554 precipitation change under global warming in the coupled model intercomparison project phase  
555 5 ensemble. *Journal of Climate*, **26** (17), 6238–6256.

556 NOAA, 2013: Defining El Niño and La Niña. Accessed: 2015-  
557 08-20, [https://www.climate.gov/news-features/understanding-climate/  
558 watching-el-nio-and-la-nia-noaa-adapts-global-warming](https://www.climate.gov/news-features/understanding-climate/watching-el-nio-and-la-nia-noaa-adapts-global-warming).

559 Oleson, K., and Coauthors, 2010: Technical description of version 4.0 of the Community Land  
560 Model (CLM). NCAR Technical Note NCAR/TN-478+STR, National Center for Atmospheric  
561 Research, Boulder, Colorado, 257 pp. doi:10.5065/D6FB50WZ.

562 Philip, S., and G. J. Van Oldenborgh, 2006: Shifts in enso coupling processes under global warm-  
563 ing. *Geophysical Research Letters*, **33** (11).

564 Pierce, D. W., 2002: The role of sea surface temperatures in interactions between enso and the  
565 north pacific oscillation. *Journal of climate*, **15** (11), 1295–1308.

566 Ralph, F. M., P. J. Neiman, and G. A. Wick, 2004: Satellite and caljet aircraft observations of  
567 atmospheric rivers over the eastern north pacific ocean during the winter of 1997/98. *Monthly  
568 Weather Review*, **132** (7), 1721–1745.

569 Rauscher, S. A., E. Coppola, C. Piani, and F. Giorgi, 2010: Resolution effects on regional climate  
570 model simulations of seasonal precipitation over Europe. *Climate dynamics*, **35** (4), 685–711.

- 571 Rauscher, S. A., T. D. Ringler, W. C. Skamarock, and A. A. Mirin, 2013: Exploring a Global  
572 Multiresolution Modeling Approach Using Aquaplanet Simulations. *Journal of Climate*, **26** (8),  
573 2432–2452.
- 574 Rhoades, A. M., X. Huang, P. A. Ullrich, and C. M. Zarzycki, 2015: Characterizing Sierra Nevada  
575 snowpack using variable-resolution CESM. *Journal of Applied Meteorology and Climatology*,  
576 (2015).
- 577 Riahi, K., and Coauthors, 2011: RCP 8.5A scenario of comparatively high greenhouse gas emis-  
578 sions. *Climatic Change*, **109** (1-2), 33–57.
- 579 Rowell, D. P., and R. G. Jones, 2006: Causes and uncertainty of future summer drying over europe.  
580 *Climate Dynamics*, **27** (2-3), 281–299.
- 581 Salathé Jr, E. P., R. Steed, C. F. Mass, and P. H. Zahn, 2008: A High-Resolution Climate Model  
582 for the US Pacific Northwest: Mesoscale Feedbacks and Local Responses to Climate Change\*.  
583 *Journal of Climate*, **21** (21), 5708–5726.
- 584 Scoccimarro, E., M. Zampieri, A. Bellucci, A. Navarra, and Coauthors, 2013: Heavy precipitation  
585 events in a warmer climate: results from CMIP5 models. *Journal of climate*.
- 586 Seneviratne, S. I., and Coauthors, 2012: Changes in climate extremes and their impacts on the  
587 natural physical environment. *Managing the risks of extreme events and disasters to advance*  
588 *climate change adaptation*, 109–230.
- 589 Sillmann, J., V. Kharin, F. Zwiers, X. Zhang, and D. Bronaugh, 2013: Climate extremes indices  
590 in the cmip5 multimodel ensemble: Part 2. future climate projections. *Journal of Geophysical*  
591 *Research: Atmospheres*, **118** (6), 2473–2493.

- 592 Simmons, A., K. Willett, P. Jones, P. Thorne, and D. Dee, 2010: Low-frequency variations  
593 in surface atmospheric humidity, temperature, and precipitation: Inferences from reanalyses  
594 and monthly gridded observational data sets. *Journal of Geophysical Research: Atmospheres*,  
595 **115 (D1)**.
- 596 Singh, D., M. Tsiang, B. Rajaratnam, and N. S. Diffenbaugh, 2013: Precipitation extremes over the  
597 continental United States in a transient, high-resolution, ensemble climate model experiment.  
598 *Journal of Geophysical Research: Atmospheres*, **118 (13)**, 7063–7086.
- 599 Staniforth, A. N., and H. L. Mitchell, 1978: A variable-resolution finite-element technique for  
600 regional forecasting with the primitive equations. *Monthly Weather Review*, **106 (4)**, 439–447.
- 601 Stevenson, S., 2012: Significant changes to enso strength and impacts in the twenty-first century:  
602 Results from cmip5. *Geophysical Research Letters*, **39 (17)**.
- 603 Stevenson, S., B. Fox-Kemper, M. Jochum, R. Neale, C. Deser, and G. Meehl, 2012: Will there  
604 be a significant change to el niño in the twenty-first century? *Journal of Climate*, **25 (6)**, 2129–  
605 2145.
- 606 Taschetto, A. S., A. S. Gupta, N. C. Jourdain, A. Santoso, C. C. Ummenhofer, and M. H. England,  
607 2014: Cold tongue and warm pool enso events in cmip5: mean state and future projections.  
608 *Journal of Climate*, **27 (8)**, 2861–2885.
- 609 Taylor, M. A., 2011: Conservation of mass and energy for the moist atmospheric primitive equa-  
610 tions on unstructured grids. *Numerical Techniques for Global Atmospheric Models*, Springer,  
611 357–380.
- 612 Tebaldi, C., K. Hayhoe, J. M. Arblaster, and G. A. Meehl, 2006: Going to the extremes. *Climatic  
613 change*, **79 (3-4)**, 185–211.

- 614 Trenberth, K. E., 2011: Changes in precipitation with climate change. *Climate Research*, **47** (1),  
615 123.
- 616 Wehner, M. F., 2013: Very extreme seasonal precipitation in the NARCCAP ensemble: model  
617 performance and projections. *Climate Dynamics*, **40** (1-2), 59–80.
- 618 Wehner, M. F., R. L. Smith, G. Bala, and P. Duffy, 2010: The effect of horizontal resolution  
619 on simulation of very extreme US precipitation events in a global atmosphere model. *Climate  
620 dynamics*, **34** (2-3), 241–247.
- 621 Wehner, M. F., and Coauthors, 2014: The effect of horizontal resolution on simulation qual-  
622 ity in the Community Atmospheric Model, CAM5.1. *J. Model. Earth. Sys.*, doi:10.1002/  
623 2013MS000276.
- 624 Yoon, J.-H., S. S. Wang, R. R. Gillies, B. Kravitz, L. Hipps, and P. J. Rasch, 2015: Increasing  
625 water cycle extremes in California and in relation to El Niño cycle under global warming. *Nature  
626 communications*, **6**.
- 627 Zarzycki, C. M., C. Jablonowski, and M. A. Taylor, 2014: Using Variable-Resolution Meshes  
628 to Model Tropical Cyclones in the Community Atmosphere Model. *Monthly Weather Review*,  
629 **142** (3), 1221–1239.
- 630 Zarzycki, C. M., C. Jablonowski, D. R. Thatcher, and M. A. Taylor, 2015: Effects of localized grid  
631 refinement on the general circulation and climatology in the Community Atmosphere Model.  
632 *Journal of Climate*, (2015).
- 633 Zhang, X., L. Alexander, G. C. Hegerl, P. Jones, A. K. Tank, T. C. Peterson, B. Trewin, and  
634 F. W. Zwiers, 2011: Indices for monitoring changes in extremes based on daily temperature and  
635 precipitation data. *Wiley Interdisciplinary Reviews: Climate Change*, **2** (6), 851–870.

636 Zhang, X., J. Wang, F. W. Zwiers, and P. Y. Groisman, 2010: The influence of large-scale climate  
637 variability on winter maximum daily precipitation over North America. *Journal of Climate*,  
638 **23 (11)**, 2902–2915.

639 update the mesh grid plot

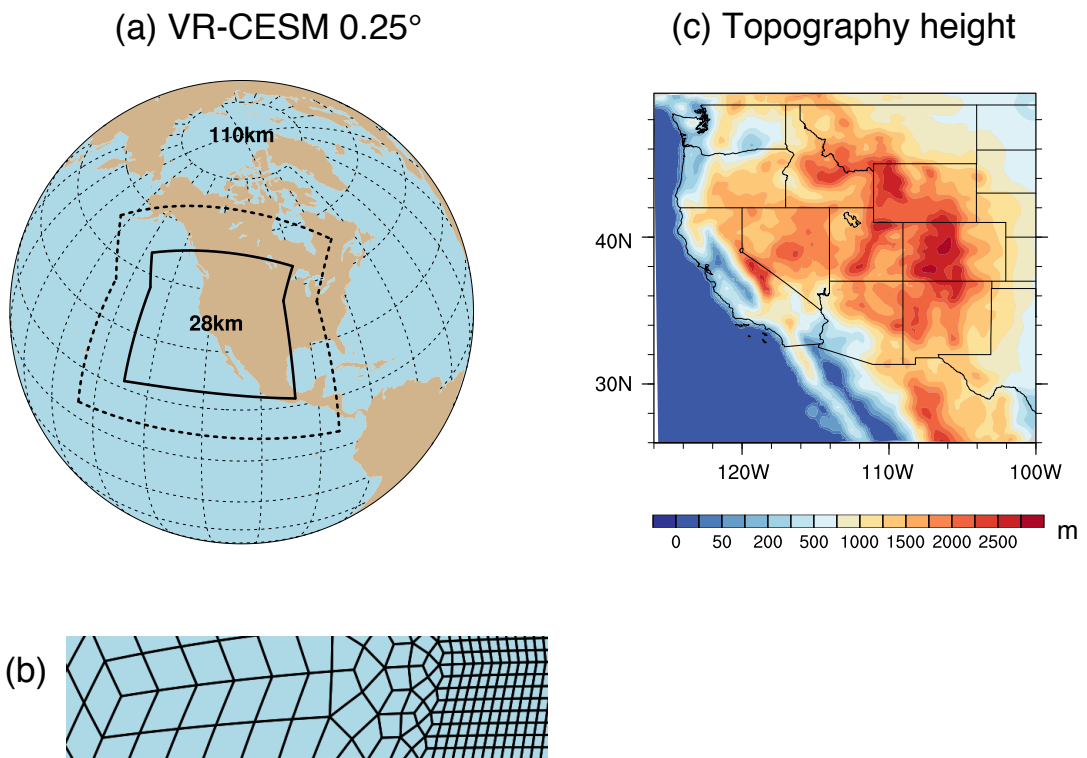
640 update the plot with new label levels

641 **LIST OF TABLES**

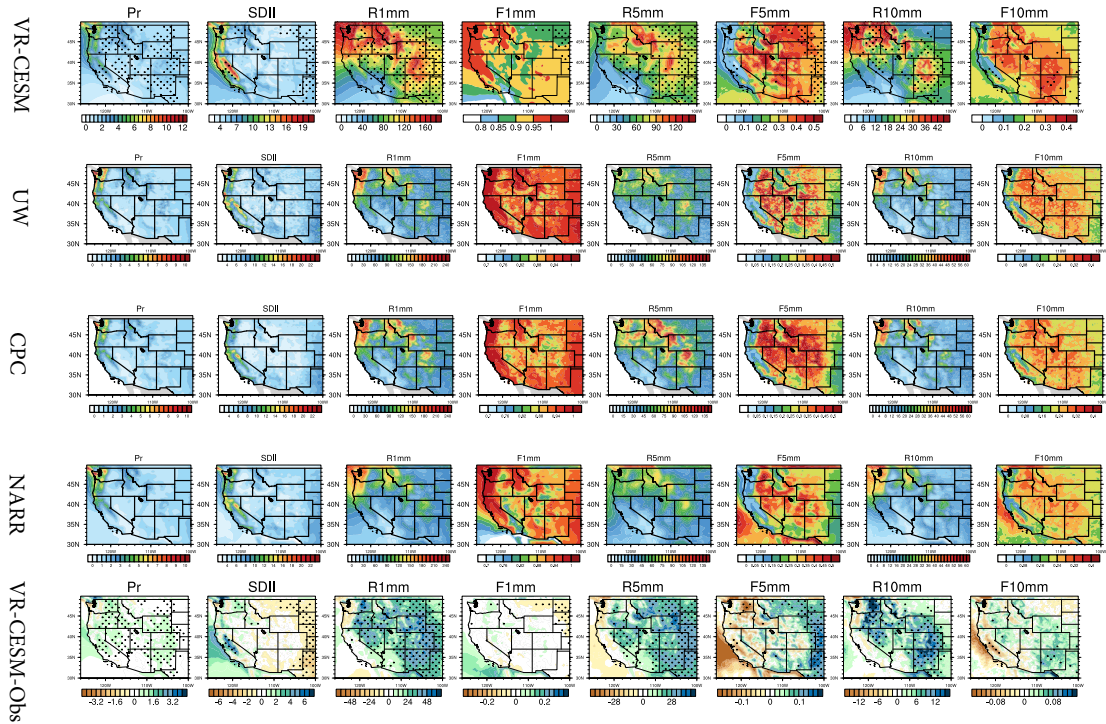
TABLE 1. Precipitation indices employed in this study.

Name	Definition
Pr	Mean daily precipitation
R1mm	Number of days per year with Pr>1 mm
SDII	Simple precipitation intensity index: Precipitation amount / $\langle R1mm \rangle$ (mm/day)
R5mm	Number of days per year with Pr>1 mm and Pr=<5 mm
R10mm	Number of days per year with Pr>5 mm and Pr=<10 mm
R20mm	Number of days per year with Pr>10 mm and Pr=<20 mm
R40mm	Number of days per year with Pr>20 mm and Pr=<40 mm
Rxmm	Number of days per year with Pr>40 mm
F1mm	Fraction of precipitation contributed to the total precipitation for days of R1mm (similarly for F5mm, F10mm, F20mm, F40mm and Fxmm)
P5mm	Precipitation amount from R5mm (similarly for P10mm, P20mm, F40mm, Pxmm)

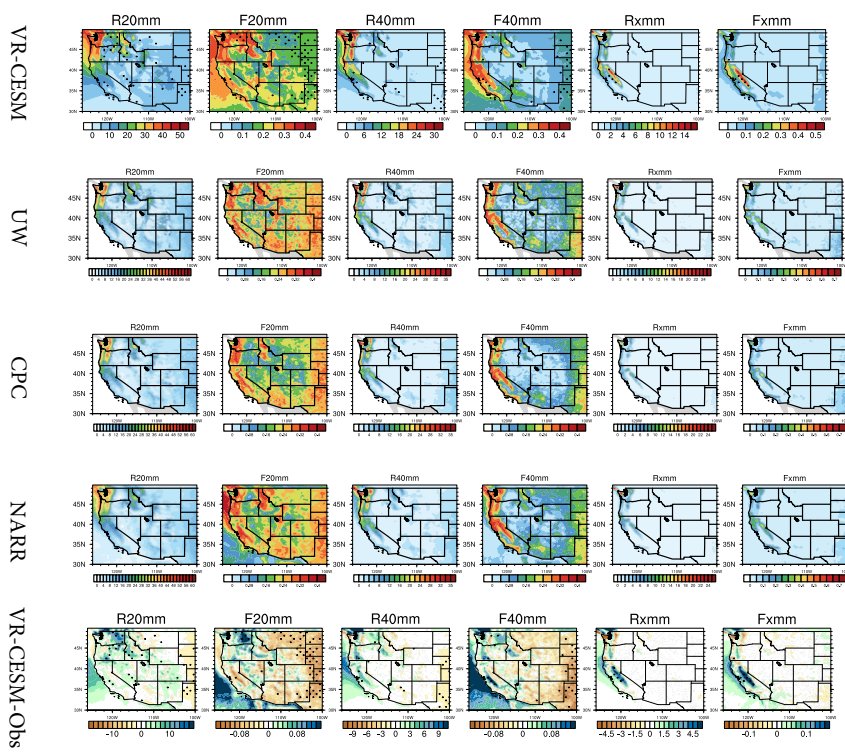
642 **LIST OF FIGURES**



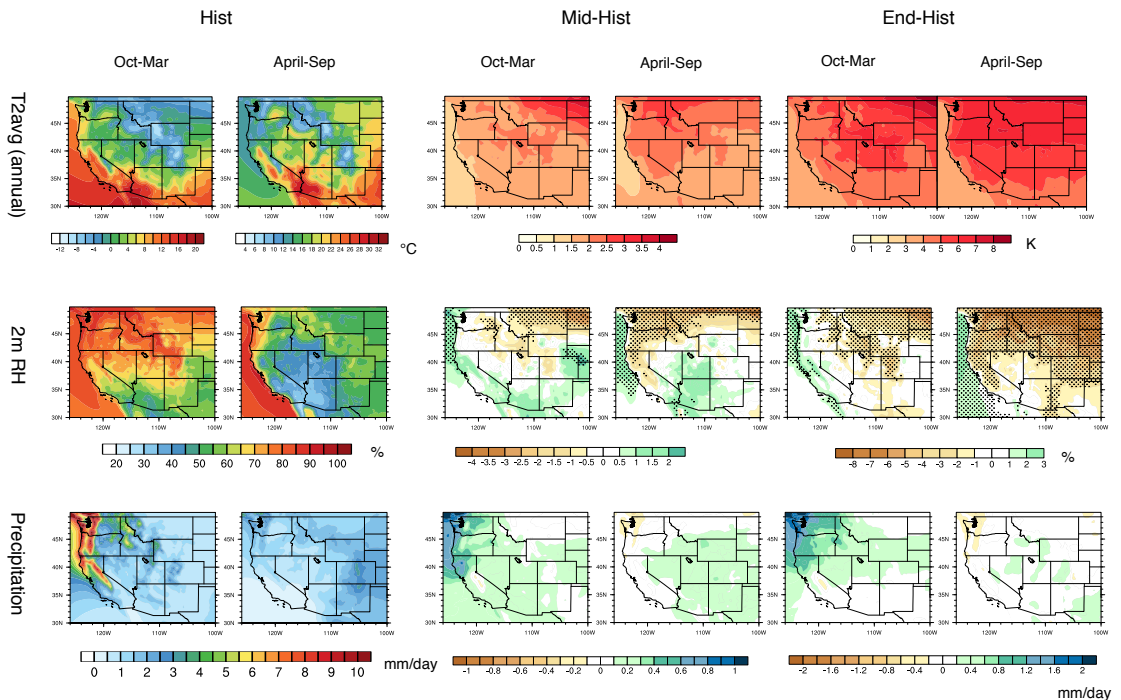
643 FIG. 1. (a) The approximate grid spacing used for the VR-CESM  $0.25^\circ$  mesh. (b) A depiction of the transition  
 644 from the global  $1^\circ$  resolution mesh through two layers of refinement to  $0.25^\circ$ . (c) Topography height over the  
 645 study area.



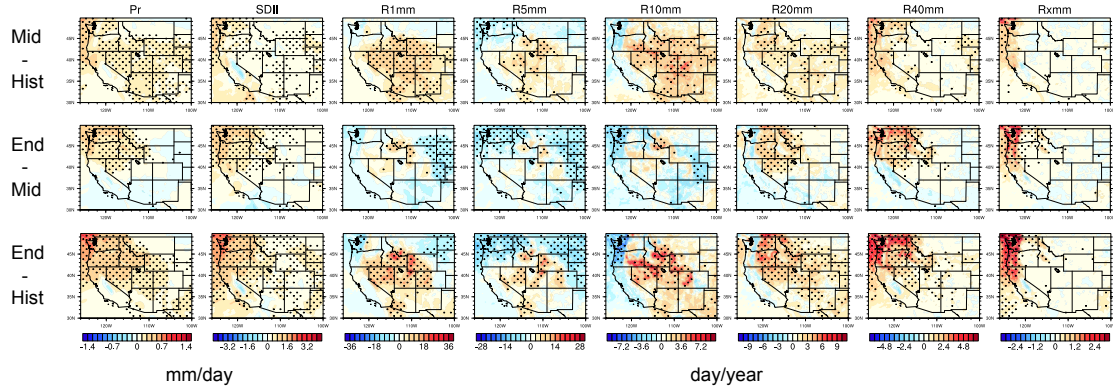
646 FIG. 2. The mean precipitation and other related indices from VR-CESM and reference datasets over 1980-  
647 2005. (Note: Grids with statistically significance difference are marked with stippling.)



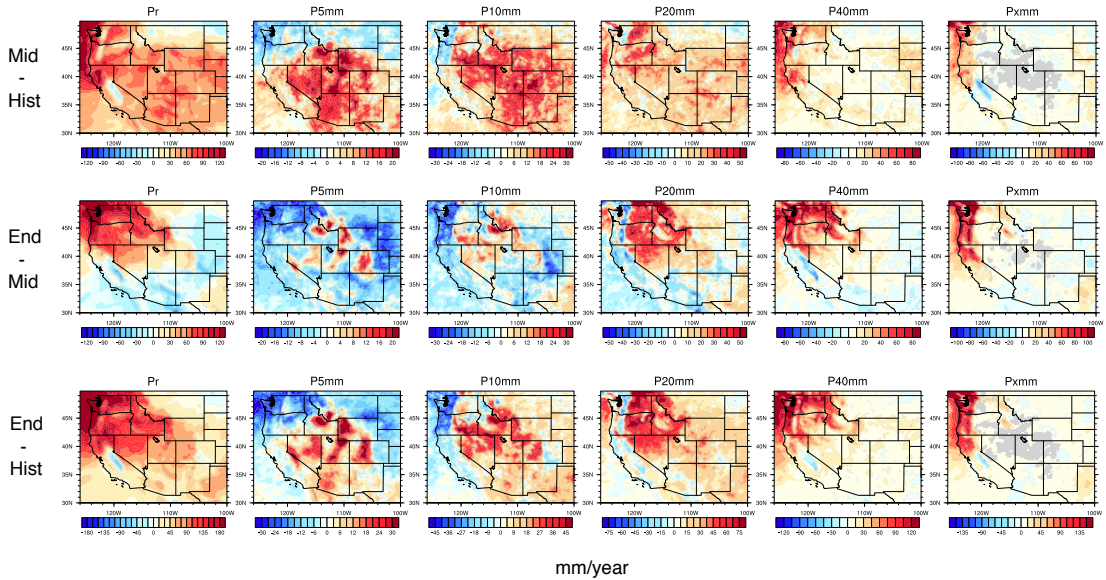
648 FIG. 3. The mean precipitation and other related indices from VR-CESM and reference datasets over 1980-  
 649 2005 (continued).



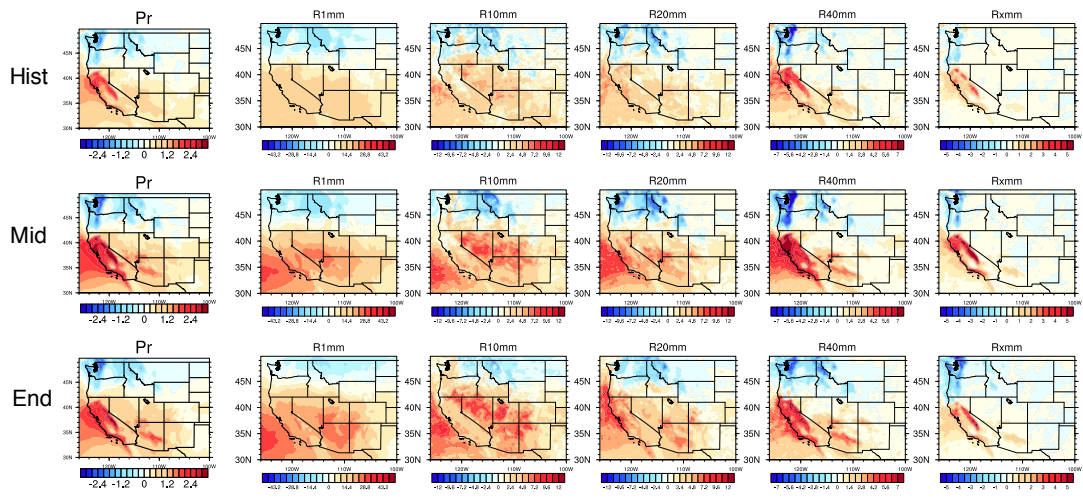
650 FIG. 4. The mean precipitation (Pr), 2m average temperature (T2avg), and 2m relative humidity (RH) aver-  
 651 aged over each time period. (Note: Grids with statistically significant difference for the RH are marked with  
 652 stippling.)



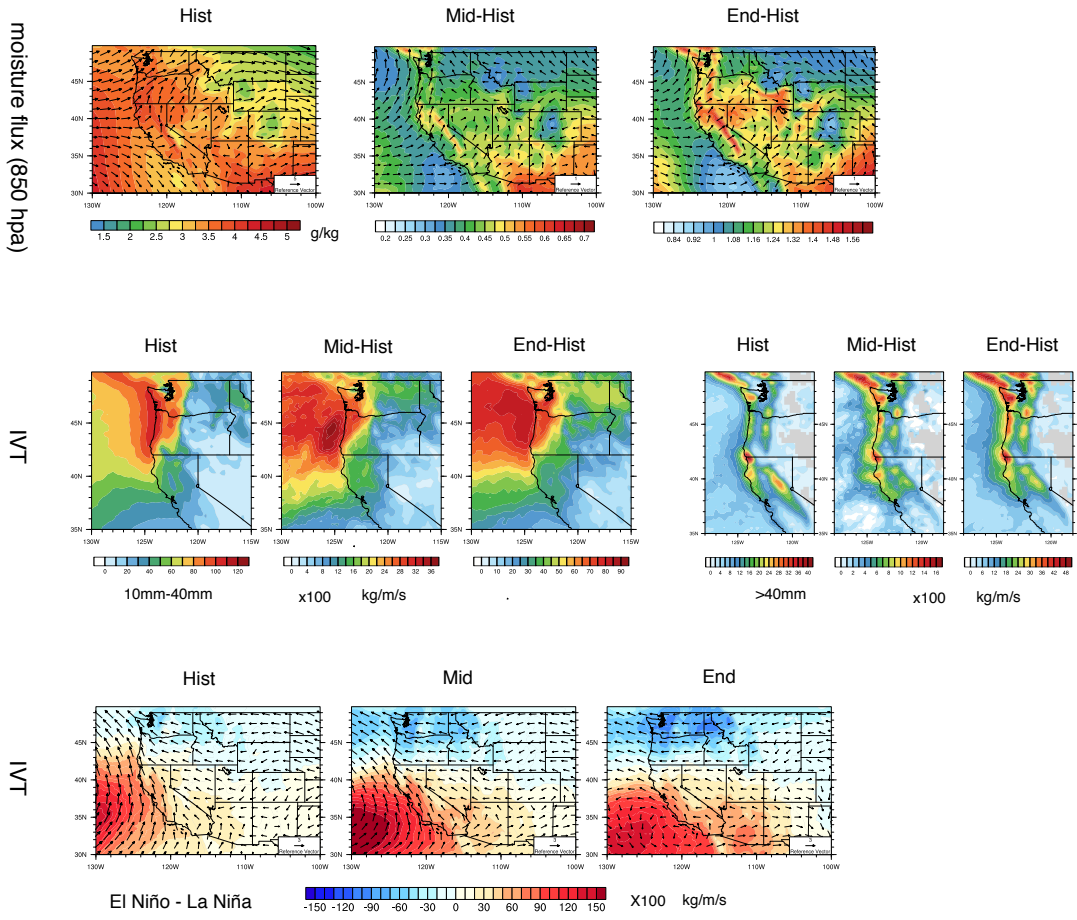
653 FIG. 5. Differences of precipitation behaviors from past to future over WUS averaged of each time period.  
 654 (Note: Grids with statistically significance difference are marked with stippling.)



655 FIG. 6. Differences of precipitation behaviors from past to future over WUS averaged of each time period  
 656 (continued).



657 FIG. 7. Difference of precipitation behaviors between warm and cool phases of ENSO from past to future  
658 over WUS averaged of each time period.



659 FIG. 8. Changes of moisture flux at 850hPa, and IVT for simulations under different time period and different  
 660 phases of ENSO of wet season (October to March). (Note: The minimum wind vector is set to be 0.5 m/s,  
 661 therefore, the wind less than 0.5 m/s is also plotted at the minimum length for better visualization.) **For all**  
 662 **difference plots, make sure to use a common [min,max] range as its currently difficult to tease out differences.**  
 663 **Difference plots should also use a different color table to the mean results (perhaps a single color color table?).**  
 664 **Remember that hectopascals is capitalized as hPa.**